Near-Infrared Spectroscopy

International Edition: DOI: 10.1002/anie.201503914
German Edition: DOI: 10.1002/ange.201503914

Organic Crystals with Near-Infrared Amplified Spontaneous Emissions Based on 2′-Hydroxychalcone Derivatives: Subtle Structure Modification but Great Property Change**

Xiao Cheng, Kai Wang, Shuo Huang, Houyu Zhang, Hongyu Zhang, and Yue Wang*

Abstract: *A series of highly efficient deep red to near-infrared (NIR) emissive organic crystals* ***1–3*** *based on the structurally simple 2′-hydroxychalcone derivatives were synthesized through a simple one-step condensation reaction. Crystal* ***1*** *displays the highest quantum yield (Φ_f) of 0.32 among the reported organic single crystals with an emission maximum (λ_{em}) over 710 nm. Comparison between the bright emissive crystals* ***1–3*** *and the nearly nonluminous compounds* ***4–7*** *clearly gives evidence that a subtle structure modification can arouse great property changes, which is instructive in designing new high-efficiency organic luminescent materials. Notably, crystals* ***1–3*** *exhibit amplified spontaneous emissions (ASE) with extremely low thresholds. Thus, organic deep red to NIR emissive crystals with very high Φ_f have been obtained and are found to display the first example of NIR fluorescent crystal ASE.*

Organic materials that exhibit efficient luminescence in the near-infrared (NIR) region have attracted much attention recently because of their potential applications in bioimaging, night vision devices, optical communication, and organic light-emitting diodes (OLEDs).[1–4] A large π-conjugated framework or strong donor–acceptor (D-A) skeleton is commonly adopted as the basic structural unit to construct NIR emitters. Thus, fluorescence quenching, the general problem for luminescent organic solids, is particularly serious for NIR fluorophores due to either attractive dipole–dipole interactions or effective intermolecular π-stacking.[5] Due to these negative influences, most of the reported efficient NIR fluorophores in dilute solutions exhibit no or weak fluorescence in solid forms.[6] These depressing results greatly obstruct the applications of NIR materials in optoelectronics including OLEDs and organic solid-state lasers (OSLs). Organic single crystals constructed from π-conjugated molecules have intrinsic properties of ordered molecular orientation and high carrier mobility, and thereby are the most likely candidates for electrically pumped organic laser materials. The lasing properties of organic crystals can be studied by means of amplified spontaneous emission (ASE). Blue to orange fluorescent organic crystals displaying the ASE property have been achieved in the past decade;[7] however, deep red and NIR-luminescent ASE-active organic crystals have not yet been reported, because it is really hard to design organic NIR-fluorescent dyes simultaneously possessing efficient solid-state emission as well as high crystallinity with suitable size and shape.

Excited-state intramolecular proton transfer (ESIPT)-active fluorophores and D-A skeletons are important components in the research area for constructing long-wavelength organic fluorescent molecules owing to their large Stokes-shifted emission.[8] And the strategies such as modulating molecular packing modes or tuning molecular conformations usually contribute to the fluorescent quantum efficiency of organic solids.[9] Following these considerations, we employ ESIPT-active and D-A structured 2′-hydroxychalcone derivatives **1–3** to construct NIR-emitting crystals (Figure 1). The

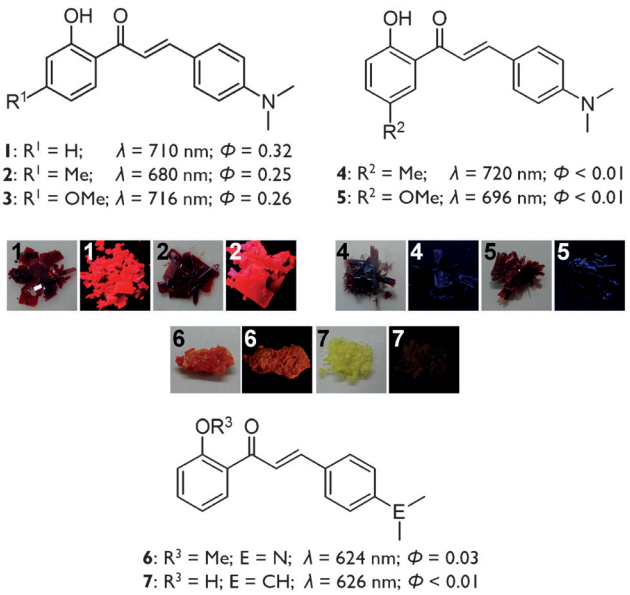

Figure 1. Molecular structures of **1–7** (the emission maxima λ and fluorescence efficiencies Φ of the solids are summarized herein) and their photographs under daylight and UV irradiation.

D-A structure, intramolecular H-bond with ESIPT nature, slip-packing structure and molecular planarization effectively make the crystals **1–3** highly emissive in the deep red/NIR region. To explore the emission mechanism of crystals **1–3**,

[*] X. Cheng, K. Wang, S. Huang, Dr. H. Zhang, Prof. Dr. H. Zhang, Prof. Dr. Y. Wang
State Key Laboratory of Supramolecular Structure and Materials
College of Chemistry, Jilin University
Qianjin Street, Changchun (P. R. China)
E-mail: hongyuzhang@jlu.edu.cn

[**] This work was supported by the National Natural Science Foundation of China (51173067 and 21221063) and the Program for Chang Jiang Scholars and Innovative Research Team in University (No. IRT101713018).

Supporting information for this article is available on the WWW under http://dx.doi.org/10.1002/anie.201503914.

the other four compounds **4**–**7** are synthesized. The optical properties as well as crystal structures have been carefully investigated. Notably, the slab-like crystals **1**–**3** display a light propagation feature and thus their potential as candidates in OSLs has been systematically investigated.

Compounds **1**–**3** are known molecules, but their optical properties are not fully investigated.[10] All the compounds are synthesized according to the literature.[11] We obtained red crystals with centimeter-scale size and slab-like shape based on **1**–**3**. As shown in Figure 1, the crystals display bright deep red to NIR fluorescence ($\lambda_{em} = 680$–716 nm; $\Phi_f = 0.25$–0.32), although their solutions are almost non-emissive ($\Phi_f < 0.01$). Additionally, these compounds display size-dependent emission in the crystalline state. For instance, the emission spectrum of **1** continually red shifts upon increasing the crystal size (Figures S2–S3). In hexane, **1** displays a local emission (LE) band peaking at 483 nm and a large Stokes-shifted emission band peaking at 542 nm which is attributed to the ESIPT-state emission (Figure 2b). Calculations on the ground state (S_0) and the lowest-energy excited singlet state (S_1) in the gas phase of **1** are conducted using the CAM-B3LYP functional. Geometry optimizations in S_1 starting from the Franck–Condon state and the proton-transferred structure give rise to two local minima corresponding to the LE and ESIPT states, respectively (Figures 2a and S4). The plausible potential energy surfaces are shown in Figure 2a. The energies of two states relative to the optimized geometry in S_0 are +3.18 and +3.11 eV with calculated emission of 414 and 475 nm, respectively, coinciding with the experimental results. In aprotic solvents, the emission spectra contain both LE and ESIPT state emission, featured as combined broad bands or dual-peak emission bands. In the protic solvent such as methanol, a narrowed emission band is observed which is assigned to the LE. Because of the D-A structure of this type of molecules, the absorption and emission bands red shift to a certain extent upon increasing the solvent polarity.

The fluorescence of crystals **1**–**3** are assigned to the tautomer produced by ESIPT which results in an abnormally large Stokes shift.[12] Considering the weak fluorescent nature of the present molecules in solution, the bright NIR fluorescence in crystals is very interesting. Thus, molecular conformations and packing structures of these crystals are crucial for understanding the bright NIR fluorescence. Crystals **1**–**3** belong to the same space group and crystal system, consistent with the similar crystal shape and fluorescence feature. As shown in Figures 3a and S5–S7, all the individual molecules take a rather planar conformation with the dihedral angle between terminal benzene rings in the range of 1.35–10.82° and show strong innate intramolecular H-bonds between the carbonyl unit and hydroxy group (1.753–1.790 Å). The strong intramolecular H-bonds greatly increase the molecular rigidity and assist in activating the molecular planarization. Each molecule in the crystal connects its neighboring molecule in an edge-to-face mode (Figure 3b), which avoids π–π interactions. Notably, the linear and flat molecules pack into infinite molecular chains

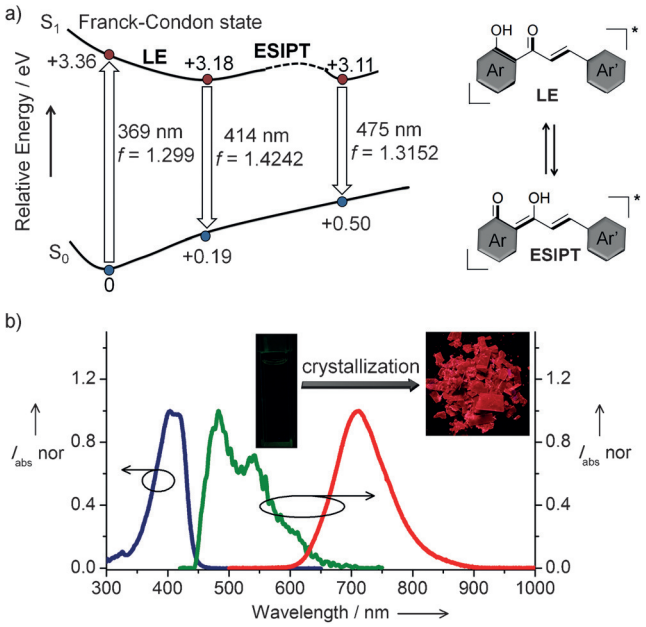

Figure 2. a) Potential energy surfaces in the gas phase and representation of the LE and ESIPT states of **1**. The relative energies calculated with the CAMB3LYP functional are given in kcal mol^{-1} relative to the optimized geometry in S_0. The TD-DFT vertical excitation energies and oscillator strengths (f) was calculated with the PBE0 functional. b) Absorption and emission in *n*-hexane (1×10^{-5} M) and crystal emission of compound **1**.

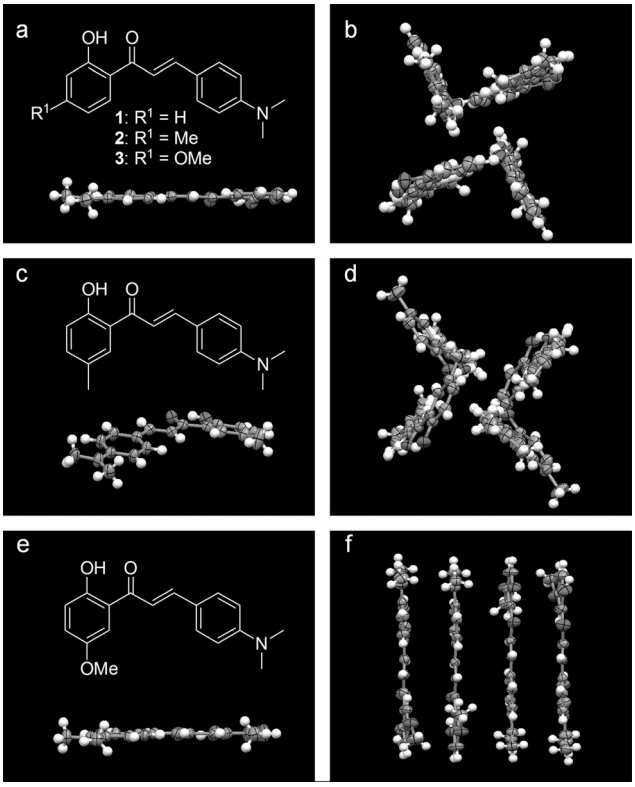

Figure 3. Molecular conformations and packing structures of crystals for **1**–**3** (a and b), **4** (c and d), and **5** (e and f).

with a typical slip-packing structure in which molecules avoid excimer formation thereby enhancing the fluorescence of solid samples. Introducing substituents such as methyl and methoxyl at the *para*-position relative to the carbonyl group does not greatly change the molecular conformation and packing mode. However, these functional groups form non-classical H-bonds which slightly alter the molecular micro-environments. Thus, the shape and fluorescence of the bulk crystals are affected in a certain degree.

The solutions under frozen condition and films of these compounds doped in polymethylmethacrylate (1–10 wt %) emit very weak fluorescence (Figure S8), demonstrating that the restriction of intramolecular rotation is likely not the key role to activate the bright light of the crystals. To further gain insights into the reason why compounds **1**–**3** are not fluorescent in dispersed states but brightly emissive in crystals, we synthesized compound **4**[13a] and obtained red slab-like crystals whose color and shape are quite similar to those of crystals **1**–**3** (Figure 1). Crystals of **4** have similar edge-to-face packing structures with **1**–**3** (Figure 3 c,d). However, the individual molecule of **4** takes a rather bent and twisted molecular conformation. This crystal is weakly fluorescent ($\lambda_{em} = 720$ nm; $\Phi_f < 0.01$) although there are no negative factors for fluorescence such as intermolecular π-stacking and dipole–dipole interactions in the crystal packing structure. This finding strongly indicates the crucial effect of molecular planarization on the fluorescence quantum yield for crystals **1**–**3**. Compound **5**[13b] is next synthesized to demonstrate the vital effect of slip-packing mode and edge-to-face arrangement structure on the high efficiency of crystals **1**–**3** (Figure 1). A similar red slab-like crystal of **5** is achieved. Nevertheless, the crystal is nearly non-emissive ($\lambda_{em} = 699$ nm; $\Phi_f < 0.01$). The molecules in crystal **5** have a relatively planar conformation (Figure 3 e), similar with those in crystals **1**–**3**. The difference of crystal structures between **5** and **1**–**3** is the molecular packing structure. As shown in Figure 3 f, unlike the edge-to-face packing mode of molecules in crystals **1**–**3**, every two molecules in crystal **5** take a face-to-face packing structure with strong π–π interactions; on the other hand, each molecule has strong dipole–dipole interactions with its neighboring molecule, which undoubtedly has an adverse effect on the quantum yield. The different packing structures make crystal **5** nearly non-emissive, whereas crystals **1**–**3** are highly fluorescent. Meanwhile, from the comparison of crystal structures among crystals **4**, **5**, and **1**–**3**, we can draw the conclusion that the molecular conformation and molecular packing structure of these molecules can be tuned by the position of the substituent. Considering the much similar molecular structures and the greatly different emission behaviors of these compounds, it is easy to find that the substituent modification has great importance on tuning the solid-state emissions of organic materials.

For a further understanding of the deep red/NIR emission of crystals **1**–**3**, 2′-methoxychalcone derivative **6**[13c] and isopropyl-substituted **7**[13d] are synthesized (Figure 1). In **6**, the hydroxy group is replaced by a methoxy group. Consequently, there is no intramolecular H-bond in compound **6**. In other words, the ESIPT process cannot occur. The isopropyl group is used in place of dimethylamino group in compound **7** to disclose the effect of strong D-A structure on the emission. The emission bands of both **6** and **7** in the solid state display a large blueshift of more than 80 nm (Figure S9) compared with **1**. This finding strongly demonstrates that the intramolecular H-bond and the D-A structure are crucially important for the deep red/NIR emission of crystals **1**–**3**. Because all those compounds have the same chalcone skeleton except for some partial changes, the distinctively different emission behaviors between **1**–**3** and **4**–**7** demonstrate that the structure modification is of great importance for organic fluorophores. This also provides an easy but effective strategy when designing new organic fluorescent materials with high efficiency in the solid state.

Crystals **1**–**3** exhibit brighter emission on edge than on their body, indicating that their emissions are highly confined inside the crystals. These observations reflect that self-waveguided emission occurs in the crystals and thus these crystals are possible candidates as organic deep red/NIR laser media. To test this possibility, one isolated single crystal of **1** is excited with a pulsed laser and the photoluminescence (PL) spectra are subsequently collected from the edge area. At low excitation power, the PL spectrum is featured as a broad emission band peaking at about 714 nm, and an amplified spontaneous emission is observed above a certain power threshold. Figure 4 a shows the power-dependent PL spectra as well as the energy dependence of the luminescence intensity and FWHM of the emissions. It shows a nonlinear gain and a threshold characteristic of ASE. The threshold of 9.2 $kW\,cm^{-2}\,pulse^{-1}$ calculated from the slope of peak intensity versus pump energy curve is among the lowest values for typical organic crystals. Thus, ASE of organic NIR-fluorescent organic crystals has been successfully realized, most importantly, having the extremely low threshold value which is a crucial parameter to evaluate the ASE property.

The ASE characteristics of the other two crystals **2** and **3** have also been checked. The thresholds of crystals **2** and **3** are 8.2 and 100 $kW\,cm^{-2}\,pulse^{-1}$, respectively. Crystal **3** displays unfavorable ASE characteristics and its PL spectra start to narrow at high excitation laser powers. This probably originates from its larger thickness compared with crystals **1** and **2** which should inevitably result in more defects in the crystal, adverse to the self-waveguided emission. To verify this, microcrystals with smaller thickness of compound **3** growing on a silicon substrate are prepared (Figure S10). The laser beam radiates on a pile of microcrystals and ASE is measured. The threshold of the microcrystals is 22 $kW\,cm^{-2}\,pulse^{-1}$, smaller than that of the normal-sized crystal **3**. In addition, the gain coefficients of crystal **1** have also been carried out by a successively variable pump stripe method in which the lengths of pump stripe are adjusted by a slit (Figure S11). The PL spectra become narrower upon increasing the pump stripe length, and this narrowing occurs more rapidly at higher pump energy, consistent with the prediction of ASE theory.[14] The polarized emission of crystal **1** is detected by using a polarizer in front of the optical fiber at the pump energy of 127 $kW\,cm^{-2}\,pulse^{-1}$. A scatterplot is shown in Figure S12, depicting the PL intensity in change of the relative angles between the crystal and the polarizer. Its

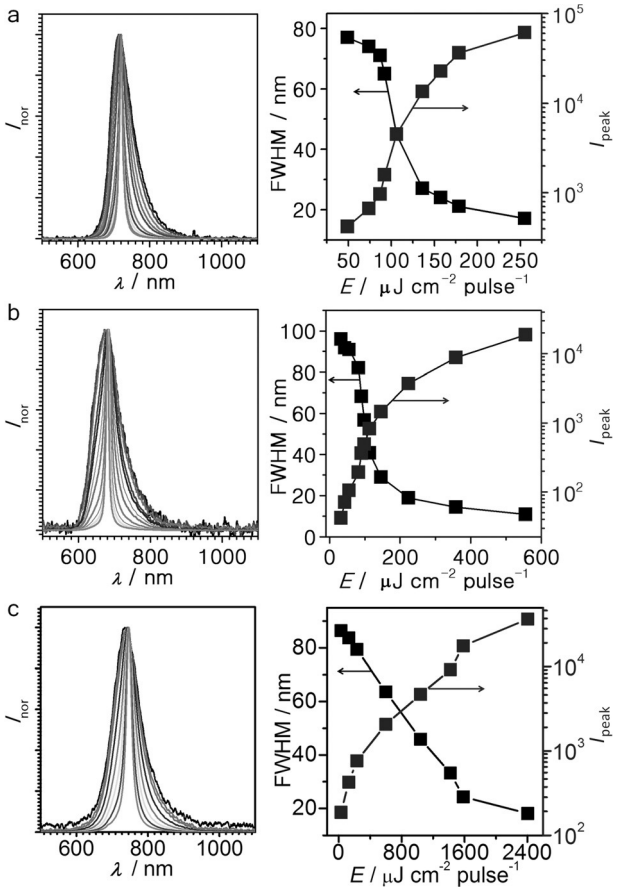

Figure 4. PL spectra as a function of the pump laser energy and dependence of the peak intensity and FWHM of emission spectra of crystal **1** (a), **2** (b), and **3** (c).

fitting curve accord with the sine function and the difference between the two angles corresponding to the maximum and minimum is close to 90°.

In conclusion, highly efficient slab-shaped deep red/NIR-fluorescent organic crystals have been generated in large amounts based on structurally simple molecules. The uniquely high quantum yield in the long-wavelength emission region of these crystals is demonstrated to originate from a combination effect of the molecular D-A structure, ESIPT-active intramolecular H-bond, molecular planarization, and the molecular packing structure without π–π interaction. Comparison between the highly efficient **1**–**3** and nearly nonluminous **4**–**7** demonstrates the partial modification of the molecular structure may play the key role in tuning the optical properties of organic fluorophores. The realization of solid-state deep red/NIR fluorescence based on simple organic dyes without large π-conjugated framework and bulky substitutions will have particular impact on design strategies toward deep red/NIR-emissive solids. These findings also exemplify how the optical properties of organic crystals can be tuned in a rational and efficient way by controlling the molecular packing mode and molecular conformation. Another significant point of the present study is that the slab-like deep red/NIR crystals exhibit ASE characters with extremely low thresholds, which suggests their possible application as organic deep red/NIR laser crystals.

Keywords: amplified spontaneous emission · near-infrared spectroscopy · organic crystals · proton transfer · π-conjugation

How to cite: *Angew. Chem. Int. Ed.* **2015**, *54*, 8369–8373
Angew. Chem. **2015**, *127*, 8489–8493

[1] a) B. N. G. Giepmans, S. R. Adams, M. H. Ellisman, R. Y. Tsien, *Science* **2006**, *312*, 217; b) T. Weil, T. Vosch, J. Hofkens, K. Peneva, K. Müllen, *Angew. Chem. Int. Ed.* **2010**, *49*, 9068; *Angew. Chem.* **2010**, *122*, 9252; c) D. Oushiki, H. Kojima, T. Terai, M. Arita, K. Hanaoka, Y. Urano, T. Nagano, *J. Am. Chem. Soc.* **2010**, *132*, 2795; d) N. Karton-Lifshin, E. Segal, L. Omer, M. Portnoy, R. Satchi-Fainaro, D. Shabat, *J. Am. Chem. Soc.* **2011**, *133*, 10960; e) X. Zhang, J. Yu, Y. Rong, F. Ye, D. T. Chiu, K. Uvdal, *Chem. Sci.* **2013**, *4*, 2143.

[2] D. Y. Kim, D. W. Song, N. Chopra, P. D. Somer, F. So, *Adv. Mater.* **2010**, *22*, 2260.

[3] a) N. Tessler, V. Medvedev, M. Kazes, S. Kan, U. Banin, *Science* **2002**, *295*, 1506; b) G. Qian, Z. Y. Wang, *Chem. Asian J.* **2010**, *5*, 1006.

[4] a) X. Du, J. Qi, Z. Zhang, D. Ma, Z. Y. Wang, *Chem. Mater.* **2012**, *24*, 2178; b) M. Casalboni, F. De Matteis, P. Prosposito, R. Pizzoferrato, *Appl. Phys. Lett.* **1999**, *75*, 2172; c) G. Qian, Z. Zhong, M. Luo, D. Yu, Z. Zhang, D. Ma, Z. Y. Wang, *J. Phys. Chem. C* **2009**, *113*, 1589.

[5] a) J. Massin, W. Dayoub, J.-C. Mulatier, C. Aronica, Y. Bretonnière, C. Andraud, *Chem. Mater.* **2011**, *23*, 862; b) O. Fenwick, J. K. Sprafke, J. Binas, D. V. Kondratuk, F. D. Stasio, H. L. Anderson, F. Cacialli, *Nano Lett.* **2011**, *11*, 2451; c) C.-K. Lim, S. Kim, I. C. Kwon, C.-H. Ahn, S. Y. Park, *Chem. Mater.* **2009**, *21*, 5819.

[6] a) J. M. Baumes, J. J. Gassensmith, J. Giblin, J.-J. Lee, A. G. White, W. J. Culligan, W. M. Leevy, M. Kuno, B. D. Smith, *Nat. Chem.* **2010**, *2*, 1025; b) Y. Koide, Y. Urano, K. Hanaoka, T. Terai, T. Nagano, *J. Am. Chem. Soc.* **2011**, *133*, 5680; c) Y.-S. Xie, K. Yamaguchi, M. Toganoh, H. Uno, M. Suzuki, S. Mori, S. Saito, A. Osuka, H. Furuta, *Angew. Chem. Int. Ed.* **2009**, *48*, 5496; *Angew. Chem.* **2009**, *121*, 5604; d) Y. Yang, M. Lowry, X. Xu, J. O. Escobedo, M. Sibrian-Vazquez, L. Wong, C. M. Schowalter, T. J. Jensen, F. R. Fronczek, I. M. Warner, R. M. Strongin, *Proc. Natl. Acad. Sci. USA* **2008**, *105*, 8829; e) S. T. Meek, E. E. Nesterov, T. M. Swager, *Org. Lett.* **2008**, *10*, 2991; f) S. Sreejith, K. P. Divya, A. Ajayaghosh, *Angew. Chem. Int. Ed.* **2008**, *47*, 7883; *Angew. Chem.* **2008**, *120*, 8001; g) U. Mayerhöffer, B. Fimmel, F. Würthner, *Angew. Chem. Int. Ed.* **2012**, *51*, 164; *Angew. Chem.* **2012**, *124*, 168.

[7] a) M. Ichikawa, R. Hibino, M. Inoue, T. Haritani, S. Hotta, T. Koyama, Y. Taniguchi, *Adv. Mater.* **2003**, *15*, 213; b) S. Park, O.-H. Kwon, S. Kim, S. Park, M.-G. Choi, M. Cha, S. Y. Park, D.-J. Jang, *J. Am. Chem. Soc.* **2005**, *127*, 10070; c) Y. Li, F. Li, H. Zhang, Z. Xie, W. Xie, H. Xu, B. Li, F. Shen, L. Ye, M. Hanif, D. Ma, Y. Ma, *Chem. Commun.* **2007**, 231; d) P. A. Losio, C. Hunziker, P. Günter, *Appl. Phys. Lett.* **2007**, *90*, 241103; e) X. Gu, J. Yao, G. Zhang, Y. Yan, C. Zhang, Q. Peng, Q. Liao, Y. Wu, Z. Xu, Y. Zhao, H. Fu, D. Zhang, *Adv. Funct. Mater.* **2012**, *22*, 4862; f) H. Wang, F. Li, I. Ravia, B. Gao, Y. Li, V. Medvedev, H. Sun, N. Tessler, Y. Ma, *Adv. Funct. Mater.* **2011**, *21*, 3770; g) Y. Wang, T. Liu, L. Bu, J. Li, C. Yang, X. Li, Y. Tao, W. Yang, *J. Phys. Chem. C* **2012**, *116*, 15576; h) M. Ichikawa, K. Nakamura, M. Inoue, H. Mishima, T. Haritani, R. Hibino, T. Koyama, Y. Taniguchi, *Appl. Phys. Lett.* **2005**, *87*, 221113.

[8] a) J. E. Kwon, S. Y. Park, *Adv. Mater.* **2011**, *23*, 3615; b) M. Shimizu, R. Kaki, Y. Takeda, T. Hiyama, N. Nagai, H. Yamagishi, H. Furutani, *Angew. Chem. Int. Ed.* **2012**, *51*, 4095; *Angew. Chem.* **2012**, *124*, 4171; c) K. Wang, H. Zhang, S. Chen, G. Yang, J. Zhang, W. Tian, Z. Su, Y. Wang, *Adv. Mater.* **2014**, *26*, 6168.
[9] a) S.-Y. Parka, M. Ebiharab, Y. Kubotaa, K. Funabikia, M. Matsui, *Dyes Pigm.* **2009**, *82*, 258; b) L. Jiao, Y. Wu, Y. Ding, S. Wang, P. Zhang, C. Yu, Y. Wei, X. Mu, E. Hao, *Chem. Asian J.* **2014**, *9*, 805.
[10] a) Z. Song, R. T. K. Kwok, E. Zhao, Z. He, Y. Hong, J. W. Y. Lam, B. Liu, B. Z. Tang, *ACS Appl. Mater. Interfaces* **2014**, *6*, 17245; b) S. Dang, J. Liu, G. Wang, *Hecheng Huaxue* **2008**, *16*, 460; c) Y. P. Kim, H. Ban, S. S. Lim, N. Kimura, S. H. Jung, J. Ji, *J. Pharm. Pharmacol.* **2001**, *53*, 1295.
[11] T. Teshima, M. Takeishi, T. Arai, *New J. Chem.* **2009**, *33*, 1393.
[12] T. Mutai, H. Tomoda, T. Ohkawa, Y. Yabe, *Angew. Chem. Int. Ed.* **2008**, *47*, 9522; *Angew. Chem.* **2008**, *120*, 9664.
[13] a) B. S. Jayashree, B. K. Kuppast, K. N. Venugopala, *Asian J. Chem.* **2007**, *19*, 1415; b) M. T. Nguyen, T. T. V. Bui, V. V. Nguyen, V. T. Nguyen, *Tap Chi Hoa Hoc* **2008**, *46*, 577; c) M. L. Edwards, D. M. Stemerick, P. S. Sunkara, *J. Med. Chem.* **1990**, *33*, 1948; d) S. V. Kostanecki, *Ber. Dtsch. Chem. Ges.* **1908**, *40*, 3669.
[14] M. D. McGehee, R. Gupta, S. Veenstra, E. K. Miller, M. A. Díza-García, A. J. Heeger, *Phys. Rev. B* **1998**, *58*, 7035.

Received: April 29, 2015
Published online: June 3, 2015

